Jurnal Teknologi

Full Paper

DESIGN, CHARACTERIZATION AND STABILITY STUDIES OF BAICALEIN LOADED CARBON NANODOTS FOR ENHANCED DRUG DELIVERY

Nasihah Mohd Zahid[a], Musbahu Adam Ahmad[b], Mochamad Zakki Fahmi[b], Nor Fazila Che Mat[a,b*]

[a]Biomedicine Programme, School of Health Sciences, Universiti Sains Malaysia, 16150 Kubang Kerian, Kelantan, Malaysia
[b]Department of Chemistry, Airlangga University, Surabaya, Jawa Timur 60115, Indonesia

Article history
Received
8 January 2025
Received in revised form
21 April 2025
Accepted
2 May 2025
Published Online
23 December 2025

*Corresponding author
fazilacm@usm.my

Graphical abstract

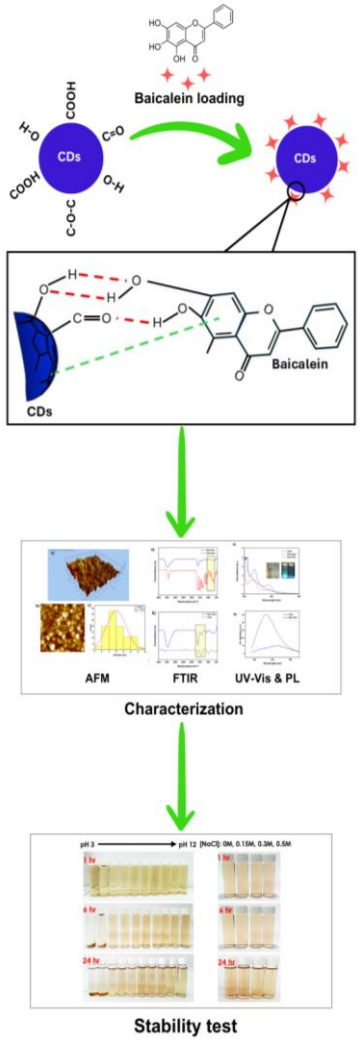

Abstract

Cancer remains a significant global health challenge, necessitating advancements in therapeutic strategies to overcome the limitations of conventional treatments, including resistance development and adverse side effects. Baicalein, a naturally derived flavonoid with potent anticancer, antioxidant, and antiinflammation properties, has shown great promise but its usage in clinical application limited by poor aqueous solubility and low bioavailability. Nanotechnology-based drug delivery systems, such as nanoparticle carbon nanodots (CDs), present a promising solution to improve drug stability, solubility, and targeted delivery. This study aimed to develop, characterize, and evaluate the stability of baicalein-loaded carbon nanodots (Bai-CDs) as a novel therapeutic delivery system. CDs were synthesized via the pyrolysis of citric acid and subsequently loaded with baicalein under optimized conditions (pH 7.4, 2:1 ratio). The resulting Bai-CDs exhibited an increase in particle size (from 10 nm to 23 nm) upon loading, with successful physical interactions confirmed by Ultraviolet-visible (UV-Vis) and Fourier Transform Infrared (FTIR) spectroscopy. The loading capacity (LC) and adsorption efficiency (AE) of baicalein were found to be 37% and 74 %. Stability assessments demonstrated the enhanced robustness of Bai-CDs under varying pH and ionic conditions, particularly in acidic environments. These findings confirm the successful design and characterization of Bai-CDs, offering improved stability and paving the way for their application as a nanocarrier system to enhance baicalein's bioavailability and therapeutic efficacy. This study underscores the potential of Bai-CDs as a promising strategy for advanced drug delivery in cancer therapy.

Keywords: Baicalein, carbon nanodots, drug delivery, cancer therapy, nanotechnology

Abstrak

Kanser telah menjadi cabaran utama dalam kesihatan global. Oleh itu, perkembangan strategi terapeutik baharu diperlukan bagi mengatasi kekangan rawatan konvensional seperti perkembangan rintangan dan kesan sampingan yang serius. Baicalein, sejenis flavonoid semula jadi yang mempunyai sifat antikanser, antioksidan, dan antiradang, telah menunjukkan potensi yang tinggi. Namun demikian, penggunaannya dalam aplikasi klinikal adalah terhad disebabkan kelarutan air yang rendah serta bio-ketersediaan yang terhad. Sistem penghantaran ubat berasaskan nanoteknologi, seperti nanopartikel karbon nanodot (CDs), menawarkan penyelesaian yang berpotensi untuk meningkatkan kestabilan, kelarutan, dan penghantaran ubat secara tersasar. Kajian ini bertujuan untuk membangunkan, mencirikan, dan menilai kestabilan baicalein yang dimuatkan pada nanopartikel karbon nanodot (Bai-CDs) sebagai sistem penghantaran terapeutik

yang inovatif. CDs dihasilkan melalui pirolisis asid sitrik, diikuti dengan proses pemuatan baicalein di bawah keadaan yang dioptimumkan (pH 7.4, nisbah 2:1). Hasilnya menunjukkan peningkatan saiz zarah Bai-CDs (daripada 10 nm kepada 23 nm) selepas pemuatan, dengan interaksi fizikal yang berjaya disahkan melalui analisis spektroskopi UV-Vis dan FTIR. Kapasiti pemuatan dan kecekapan penyerapan baicalein masing-masing adalah sebanyak 37% dan 74%. Penilaian kestabilan menunjukkan bahawa Bai-CDs mempunyai ketahanan yang lebih baik dalam pelbagai keadaan pH dan ionik, terutamanya dalam persekitaran berasid. Penemuan ini mengesahkan kejayaan reka bentuk dan pencirian Bai-CDs, di samping menunjukkan peningkatan kestabilan, yang berpotensi digunakan sebagai sistem pembawa nano untuk meningkatkan bio-ketersediaan dan keberkesanan terapeutik baicalein. Kajian ini menggariskan potensi Bai-CDs sebagai pendekatan baharu yang menjanjikan dalam penghantaran ubat bagi terapi kanser yang lebih berkesan.

Kata kunci: Baikalein, nanodot karbon, penghantaran ubat, terapi kanser, nanoteknologi

1.0 INTRODUCTION

Cancer continues to be a major global health challenge, ranking among the leading causes of mortality worldwide, with millions of new cases and deaths reported annually [1]. Conventional cancer treatment strategies, including chemotherapy, radiotherapy, and surgery, have achieved significant success in prolonging survival and improving the quality of life for patients. However, these treatments are often accompanied by considerable limitations. Chemotherapy, in particular, relies on synthetic drugs to inhibit cancer cell proliferation or induce apoptosis [2]. Despite its effectiveness in targeting rapidly dividing cancer cells, chemotherapy is inherently non-specific, often affecting healthy cells and tissues [3]. This lack of specificity frequently leads to severe side effects, including nephrotoxicity, cardiotoxicity, infertility, and immune suppression, ultimately reducing the overall quality of life for patients [4], [5]. Such challenges have prompted researchers to seek alternative therapeutic strategies that are both effective and less toxic [4].

Natural products have gained significant attention as alternative or complementary anticancer agents due to their inherent therapeutic potential, minimal side effects, and diverse pharmacological activities [6]. Among these, baicalein, a naturally occurring flavonoid derived from medicinal plants such as *Oroxylum indicum* and *Scutellaria baicalensis*, has shown promise as a potent anticancer compound. Baicalein exhibits broad-spectrum anticancer activity through multiple mechanisms, including the induction of apoptosis, inhibition of angiogenesis, suppression of tumor cell proliferation, and modulation of various signaling pathways involved in cancer progression [7]–[10]. Additionally, its antioxidant and anti-inflammatory properties further enhance its therapeutic potential. The favorable safety profile of baicalein makes it an attractive candidate for drug development. However, its clinical translation has been significantly hindered by its poor water solubility, rapid metabolism, and low oral bioavailability, which limit its systemic circulation and therapeutic efficacy [11].

Nanotechnology has emerged as a transformative tool in drug delivery, offering innovative solutions to overcome the limitations of conventional therapies and natural compounds. Among various nanocarriers, nanoparticle carbon nanodots (CDs) have garnered significant attention due to their unique physicochemical properties. CDs are small, biocompatible nanoparticles characterized by their low cytotoxicity, high water solubility, tunable surface chemistry, and intrinsic fluorescence [12]. These properties make them ideal candidates for drug delivery applications. CDs can encapsulate or load therapeutic agents like baicalein, protecting them from enzymatic degradation and improving their solubility and stability. Furthermore, the ability to functionalize CDs with specific ligands or targeting molecules enables precise delivery to cancer cells, thereby enhancing therapeutic efficacy while minimizing off-target effects and systemic toxicity [13], [14].

The synergistic combination of baicalein and CDs represents a promising approach to address the shortcomings of both natural compounds and conventional cancer treatments. By leveraging the drug delivery capabilities of CDs, the therapeutic index of baicalein can be significantly improved, allowing for targeted delivery, sustained release, and enhanced bioavailability. Recent studies have highlighted the potential of this combination in improving drug stability, reducing off-target effects, and enhancing anticancer efficacy. Additionally, the fluorescence properties of CDs offer opportunities for simultaneous therapeutic and diagnostic applications, a concept known as theranostics, further expanding their utility in oncology [15].

This study aims to develop, characterize, and evaluate the stability of Bai-CDs as a novel drug delivery system for cancer therapy. By designing Bai-CDs with optimal physicochemical properties, including size and surface functionality, this research focuses on achieving effective drug loading and

controlled release. Advanced analytical techniques, such as Ultraviolet-visible (UV-Vis) spectroscopy, fluorescence spectroscopy, Fourier-transform infrared (FTIR) spectroscopy, and Atomic Force Microscope (AFM) will be employed to confirm the physical combination of baicalein and CDs, providing detailed insights into their structural and functional attributes. Stability studies will further assess their robustness under various environmental and physiological conditions, ensuring their suitability for clinical applications. These findings represent the first confirmation of the successful design, characterization, and stability of this novel baicalein-CDs system, paving the way for improved bioavailability and less toxic, targeted cancer therapies.

2.0 METHODOLOGY

2.1 Synthesis of Carbon Nanodots (CDs)

Nanoparticle carbon nanodots were synthesized using citric acid as the precursor. Briefly, CDs were prepared by weighing 100 mg of citric acid and placed in glass vials. The samples were placed in a furnace oven (Thermo Scientific F6010 Thermolyne Furnace A1, 14L, 3095 W) and pyrolyzed for 2 hours (H) at a temperature exceeding 200°C. The resulting products were dissolved in 1 mL of 2 M NaOH solution and sonicated to ensure thorough dispersion. The resulting dark concentrated solution was centrifuged to remove large particulate impurities, yielding a brownish solution. The CDs solution was further dried using convection heating to obtain solid powders. The final CDs were stored at 4°C for subsequent analyses and applications.

2.2 Baicalein loading onto CDs

Bai-CDs were prepared as follows: A baicalein solution (5 mg/mL) was prepared by dissolving baicalein powder in a mixture of dimethylformamide (DMF) and phosphate-buffered saline (PBS) in a 1:1 ratio. Separately, a carbon nanodots solution (5 mg/mL) was prepared. The CDs solution and baicalein solution were mixed in a 2:1 ratio, and the pH of the combined solution was adjusted to 7.4. The solution was stirred overnight at room temperature in the dark to ensure effective interaction and proper loading of the baicalein onto the nanoparticles. Following overnight stirring, the solution was subjected to ultrasonication at 50% amplitude for 2–4 minutes to help achieve a well-dispersed, stable, and homogenous solution. The solution was then observed for any precipitation, and the combined nanoparticles were purified by dialysis against distilled water, and solid powders were obtained by lyophilization.

Additionally, the adsorption efficiency (AE) and loading capacity (LC) of baicalein on the CDs were calculated to evaluate the effectiveness of baicalein loading. AE represents the percentage of baicalein successfully adsorbed onto the CDs relative to the initial amount used, while LC indicates the proportion of baicalein in the final Bai-CDs formulation. The following equations were used:

(1) Adsorption efficiency (%)= [(mass of Baicalein on CDs/(mass of Baicalein in feed)]x 100 [16]

(2) Loading capacity (%)= [(mass of Baicalein on CDs)/(mass of CDs)] X 100 [16]

2.3 Physicochemical and Characterization Properties

Morphology of CDs and Bai-CDs observed atomic force microscopy (AFM 5500M, Japan). The diameter of CDs and Bai-CDs were calculated from AFM images using Origin and IMAGE J analysis software. The sample function group was determined using Fourier transform infrared spectrometer (FTIR, Shimadzu IR Tracer-199, Japan). UV-vis absorption spectra were measured using a UV-vis spectrophotometer (SHIMADZU 1800, Japan). PL spectra of the nanoparticles were measured using a spectrofluorometer (PerkinElmer LS 55, USA) equipped with a 20kW xenon lamp with a quartz cuvette having a 0.5 cm path length.

2.4 Stability Test

The stability of Bai-CDs in aqueous solutions was evaluated by observing their appearance across different pH levels and ionic strengths. Bai-CDs were prepared at a fixed concentration and adjusted to pH values ranging from 3 to 12 using appropriate buffer solutions. Additionally, solutions were prepared with varying ionic strengths by adding sodium chloride, (NaCl) at concentrations of 0 M, 0.15 M, 0.3 M, and 0.5 M. The solutions were visually inspected for any signs of precipitation, colour changes, or turbidity at intervals 1, 6, and 24 H. Turbidity value of colloidal nanoparticles was measured by TB1 portable turbidimeter (VELP Scientifica, Italy). To further analyze stability, UV-Vis spectroscopy was performed at each time point to detect changes in absorbance peaks, particularly those below 300 nm, these peaks were monitored for intensity reductions or shifts, indicating possible aggregation or structural instability. The effects of both pH and ionic strength on the stability of Bai-CDs were carefully assessed to understand their behavior under different environmental conditions.

3.0 RESULTS AND DISCUSSION

3.1 Synthesis of Nanoparticles

Upon pyrolyzing citric acid at temperatures exceeding 200°C, a distinct colour change was observed in the reaction mixture, transitioning from a transparent/white to a dark brown concentrated liquid. This colour change is indicative of the formation of CDs, which is attributed to the carbonization process and the generation of conjugated π-systems. After dispersion in 2 M NaOH and subsequent purification via centrifugation, the resulting brownish solution exhibited strong fluorescence under UV light, suggesting successful synthesis of fluorescent CDs (Figure 1).

The visual and fluorescent changes are characteristic of CDs due to the presence of surface functional groups and quantum confinement effects, as supported by previous studies [17], [18]. The addition of baicalein to the CDs solution resulted in noticeable changes to the solution's appearance. The initial yellowish/brownish solution of CDs became slightly darker upon mixing with the baicalein solution. This colour change, followed by overnight stirring and ultrasonication, suggests successful interaction between baicalein and the surface of the CDs.

Figure 1 Bai-CDS solution exhibited darker brownish solution (left) and CDs solution showed bright green fluorescence under UV light (right), confirming successful synthesis

3.2 Characterization Properties

3.2.1 Structural and Morphological Properties (AFM)

Atomic Force Microscopy was employed to examine the morphological characteristics and size distribution of the nanomaterials. The particle size distributions of CDs and Bai-CDs were analyzed using IMAGE J and Origin software, as depicted in Figure 2 and 3. The analysis revealed that the average particle sizes for CDs and Bai-CDs were 10.02 nm and 23.34 nm, respectively. The AFM analysis of CDs revealed a relatively uniform size distribution, with an average diameter of approximately 10 nm, consistent with the nanoscale dimensions typical of nanoparticle carbon nanodots (Figure 2 and 3) [19]–[21]. Upon loading baicalein onto the CDs, an increase in the average particle size was observed in the Bai-CDs sample, with diameters reaching up to 23 nm (Figure 3). This notable size increase indicates the successful combination of the CDs, where baicalein molecules were effectively loaded onto their surface, forming larger nanocomposites. These findings align with previous studies, which reported that the combination or loading of small molecules onto nanoparticle surfaces often results in an increase in particle size [22].

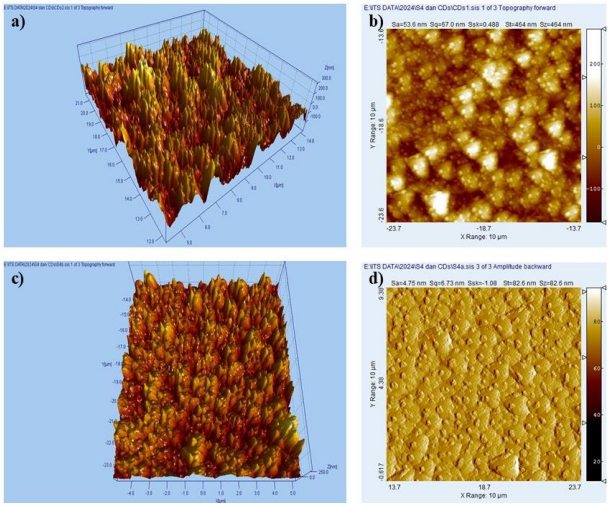

Figure 2 (a) 3D and (b) 2D morphologies of CDs, and (c) 3D and (d) 2D morphologies of Bai-CDs obtained from AFM analysis

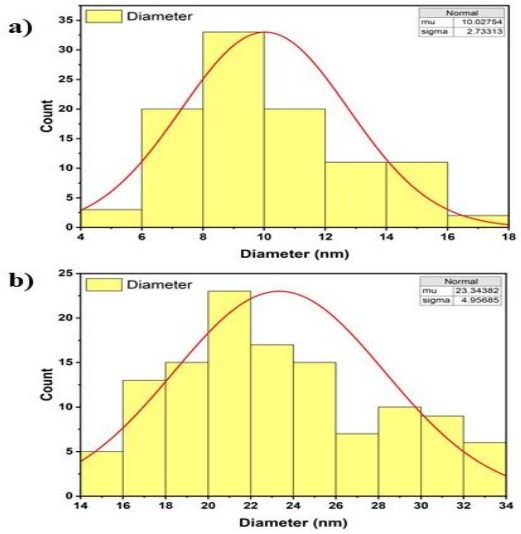

Figure 3 Size distribution of CDs (a) and Bai-CDs (b)

3.2.2 Optical Properties (UV-Vis and PL)

The UV-Vis absorption spectra of CDs, baicalein, and Bai-CDs is shown in Figure 4(a). The spectrum of CDs (black line) shows a characteristic shoulder peak at around 240–280 nm, which is attributed to π−π* transitions of C=C bonds in the aromatic sp^2 domains. Additionally, the weaker absorbance extending into the visible region suggests n−π* transitions of C=O bonds or other oxygen-containing functional groups

on the surface of the CDs, indicating the presence of functionalized groups that contribute to their electronic properties [23], [24]. The spectrum of baicalein (red line) exhibits a strong absorption peak around 250–320 nm, corresponding to π–π* transitions within its aromatic rings and conjugated systems [25]. A smaller shoulder in the 330–350 nm range likely arises from n–π* transitions involving functional groups such as hydroxyl (-OH) or carbonyl (C=O) groups present in baicalein's structure. This spectrum reflects the characteristic electronic transitions associated with baicalein's bioactive functional groups [25], [26].

In the case of Bai-CDs (blue line), the spectrum combines features of both CDs and baicalein, with significant broadening and shifts in the absorption maximum. A prominent absorption peak or shoulder around 270–280 nm indicates enhanced π–π* interactions between baicalein and the aromatic sp^2 domains of the CDs. The broadening of peaks and the emergence of a distinct absorption band extending into the 300–400 nm range suggest the formation of a combination system or charge-transfer interactions between baicalein and the surface functional groups of the CDs. These spectral changes imply that baicalein is successfully bound or physically interact onto the CDs, resulting in new electronic transitions. The observed shifts and broadened peaks provide strong evidence of physical interactions between baicalein and CDs, which may include π–π stacking interactions between the aromatic regions of baicalein and the sp^2 domains of CDs, hydrogen bonding between baicalein's hydroxyl groups and oxygen-containing functional groups on the CDs that enhance the overall absorption profile.

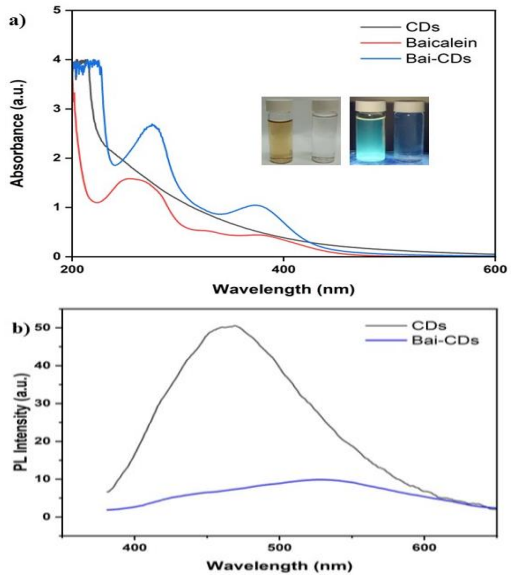

Figure 4 (a) UV-Vis absorption spectra of CDs (black line), baicalein (red line), and Bai-CDs (blue line). The inset shows photographic images of the CDs and distilled water (control) under different lighting conditions. On the left, the samples are shown under visible light, with no fluorescence observed. On the right, the green fluorescence emitted by the CDs is clearly visible under UV light at λmax 365 nm, while the control remains non-fluorescent. (b) Fluorescence excitation spectra of CDs (black line) and Bai-CDs (blue line).

The fluorescence emission spectra, Figure 4(b) demonstrate significant differences between the CDs and the Bai-CDs combination. CDs (black line) alone exhibit strong fluorescence emission in the visible range at 465 nm, consistent with their known photoluminescent properties, likely due to the presence of functional groups that enhance fluorescence quantum yield. In the Bai-CDs sample (blue line), fluorescence quenching is observed compared to the CDs alone. This reduction in photoluminescence intensity suggests that baicalein is interacting with the CDs, potentially via non-radiative energy transfer mechanisms or electron transfer from the excited states of CDs to baicalein [26]. The quenching effect aligns with observations from other studies on nanomaterial-flavonoid systems, where fluorescence intensity decreases as a result of energy transfer between the nanoparticle and the loaded molecule [22], [27]–[30].

3.2.3 *Surface Chemistry (FTIR)*

Figure 5 shows the FTIR spectra of pure baicalein, CDs, and Bai-CDs. The characteristic peaks property of pure baicalein (red line) was exhibited at 3408.4 cm^{-1} (O – H stretching) and 1654.57 cm^{-1} (C = O stretching). It also showed peak at 1080 cm^{-1}, corresponding to C –O stretching vibration. These peaks collectively confirm the phenolic and flavonoid structure of baicalein [31].

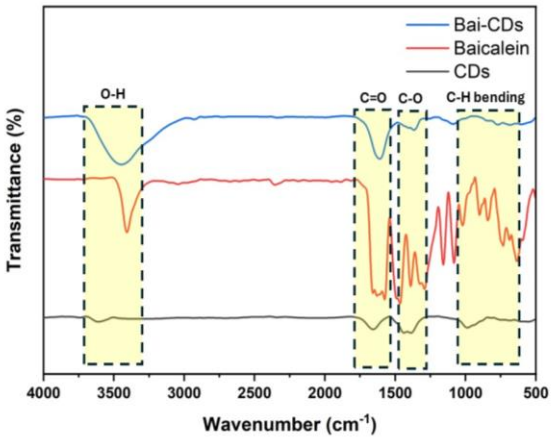

Figure 5. FTIR spectra of Bai-CDs (blue line), Baicalein (red line), and CDs (black line). Characteristic absorption peaks corresponding to functional groups are highlighted: broad O–H stretching, C=O stretching, C–O stretching, and C–H bending. The appearance of these peaks in Bai-CDs confirms the successful incorporation of Baicalein functional groups onto CDs surface, indicating effective surface functionalization during synthesis

For CDs (black line), the absorption peaks showed at 3608 cm^{-1} (O – H stretching), 1656 cm^{-1} (C = C stretching), 1383 cm^{-1} (C – O stretching or C–H bending vibrations) and multiple peaks at below 1000 cm^{-1} wavenumbers, indicating the presence of a benzene group on the CDs surface [32]. In the Bai-

CDs (blue line) spectrum, shifts in the C=O and O-H stretching frequencies are observed, suggesting that baicalein interacts with the surface of the CDs, likely through hydrogen bonding or π-π stacking interactions (Figure 6). Additionally, the peak at 1090 cm^{-1}, which corresponds to C-O stretching, appears in both the Bai-CDs and baicalein spectra. These results and shifts demonstrate that no new chemical bonds were formed; however, it become indicative of physical binding between the surface functional groups of the CDs and baicalein, which alters the vibrational energy levels of the molecules [31].

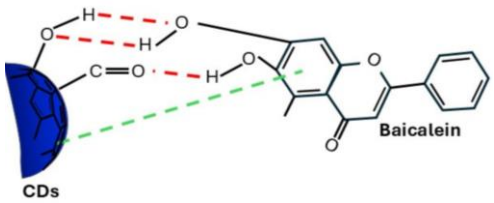

Figure 6 Schematic representation of the interaction between baicalein and CDs through hydrogen bonding (red dashed lines) and π–π stacking interactions (green dashed lines), indicating non-covalent physical binding

3.3 Stability Evaluation of the Nanoparticles

In drug delivery systems, stability refers to the ability of nanoparticles to remain uniformly dispersed, structurally intact, and functionally effective over time under various physiological and environmental conditions. Good stability is typically characterized by minimal aggregation or precipitation, consistent particle size, low turbidity, and a stable surface charge, which is commonly indicated by a zeta potential exceeding ±30 mV. These characteristics ensure that the formulation maintains its therapeutic efficacy across a broad pH range (ideally pH 4–9) and within physiologically relevant salt concentrations (0.15–0.5 M NaCl) [33], [34]. This stability supports predictable and sustained drug release, enhancing the formulation's suitability for biological applications.

Conversely, poor stability manifests as rapid aggregation, visible precipitation, increased turbidity, size fluctuations, or chemical degradation, all of which may result in premature drug release, reduced bioavailability, and diminished therapeutic performance. In this study, the colloidal stability of CDs and Bai-CDs under varying pH and ionic strength conditions was systematically evaluated through a combination of visual observations (Figure 7), UV–Vis spectroscopy (Figures 9 and 11), and turbidity measurements (Figures 8 and 10). Stability assessments were conducted at multiple time points; 1 hour (1 H), 6 hours (6 H), and 24 hours (24 H) to monitor the temporal evolution of nanoparticle dispersion and aggregation.

Turbidity measurements provided a quantitative evaluation of colloidal behavior, where higher turbidity values indicated increased nanoparticle aggregation and reduced stability. The results revealed both shared and distinct stability profiles between CDs and Bai-CDs, offering valuable insights into their respective stabilization mechanisms.

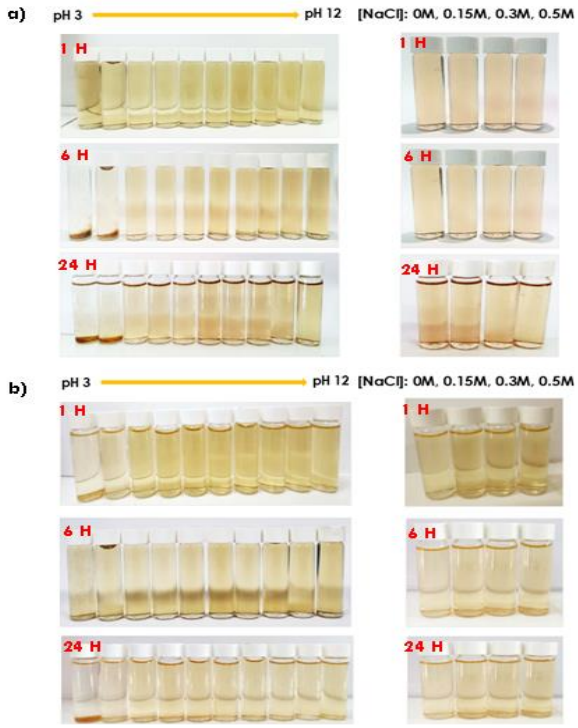

Figure 7 Photograph images of CDs from pH 3 to pH 12 and 0 M, 0.15 M, 0.3 M, and 0.5 M of NaCl at 1 H, 6 H, and 24 H (a). Photograph images of Bai-CDs from pH 3 to pH 12 and 0 M, 0.15 M, 0.3 M, and 0.5 M of NaCl at 1 h, 6 H, and 24 H (b)

3.3.1 Stability Under pH Variations

By referring to Figure 7(a), the CDs displayed remarkable stability across a pH range of 5–12, retaining their brown-yellowish colour without visible aggregation or precipitation. However, at pH 3 and 4, significant instability was observed, with precipitation forming within 6–24 H. This instability can be attributed to the protonation of functional groups on the CD surface at low pH, which weakens electrostatic repulsion and leads to particle aggregation [35]. CDs exhibited good colloidal stability across the pH range of 5 to 12 at all time points, as reflected by consistently low turbidity values and stable UV–Vis absorbance spectra (Figures 8(a–c) and 9(a–c)). However, under acidic conditions (pH 3 and 4), pronounced instability was observed. At 1 H, turbidity increased significantly—13 NTU at pH 3 and 7 NTU at pH 4 (Figure 8(a)), indicating early-stage aggregation. This pattern persisted at 6 H (Figure 8(b)), with sustained high turbidity at pH 3 (~12 NTU), and was still evident at 24 H (~11 NTU, Figure 8(c)), suggesting long-term instability in strongly acidic environments.

These findings were supported by UV–Vis data, which showed a marked decrease in absorbance at pH 3 and 4 over time (Figures 9(a–c)), consistent with particle aggregation and sedimentation. This instability likely results from protonation of surface functional groups at low pH, which reduces electrostatic repulsion and promotes aggregation [35]. Conversely, the spectra between pH 5 and 12 remained largely unchanged, indicating good structural integrity and dispersion stability in neutral to alkaline conditions.

In comparison, Bai-CDs (Figure 7(b)) demonstrated enhanced stability over a broader pH range (4–12), surpassing the performance of unmodified CDs. At 1 H, turbidity was elevated at pH 3 (~26 NTU) yet remained lower and more consistent across pH 4 to 12 (~15–20 NTU) (Figure 10(a)), suggesting better initial dispersion. By 6 H, turbidity at pH 3 remained high (~25 NTU), while values at pH 4 to 6 showed modest improvement (~17–19 NTU) (Figure 10(b)). Notably, at 24 H, Bai-CDs maintained colloidal stability from pH 4 to 12, with turbidity values declining further, especially under basic conditions (Figure 10(c)). For example, turbidity at pH 8–12 dropped below 10 NTU, indicating strong long-term dispersion in environments relevant to physiological pH [36].

This trend was corroborated by UV–Vis spectra (Figures 11(a–c)), where minimal spectral shifts were observed at pH 4–12, supporting good optical and structural stability. However, at pH 3, a visible reduction in absorbance was noted, particularly at 24 H (Figure 11(c)), implying some degree of aggregation. The partial mitigation of pH-induced aggregation in Bai-CDs is attributed to the steric stabilization imparted by baicalein, which enhances resistance against surface protonation and interparticle interactions [37].

3.3.2 Stability Under Ionic Strength Conditions

Both CDs and Bai-CDs exhibited exceptional stability across a range of NaCl concentrations (0–0.5 M), with no visible aggregation or precipitation observed in visual inspections (Figure 7), even at the highest salt concentration tested. This indicates strong resistance to salt-induced destabilization for both nanoparticle systems, although the underlying stabilization mechanisms differ. In the case of CDs, stability is primarily governed by electrostatic repulsion between surface-charged functional groups. For Bai-CDs, baicalein contributes an additional steric barrier that helps resist ionic compression effects, thus enhancing colloidal stability under high-salt conditions [37].

For CDs, turbidity values remained remarkably low across all time points and salt concentrations (Figures 8(d–f)). At 1 H, turbidity increased only slightly from ~0 NTU (0 M) to ~1.1 NTU at 0.5 M NaCl (Figure 8(d)). By 6 H, a minor elevation (~2.3 NTU) was noted at 0.5 M (Figure 8(e)), and this trend persisted slightly at 24 H (~1.6 NTU, Figure 8(f)). These modest increases suggest minimal ionic interaction and confirm that the colloidal dispersion remained largely unaffected by salt-induced screening.

Correspondingly, UV–Vis spectra of CDs (Figures 9(d–f)) showed no significant spectral shifts or absorbance loss across all NaCl concentrations and time points, indicating that their electronic structure and surface chemistry remained intact. This confirms the robustness of electrostatic stabilization mechanisms in maintaining colloidal integrity under ionic stress.

Similarly, Bai-CDs demonstrated excellent tolerance to increasing NaCl concentrations, supported by consistent turbidity profiles and stable spectral behaviour. At 1 H, turbidity values ranged slightly higher, from ~19 NTU at 0 M to ~21 NTU at 0.5 M (Figure 10(d)). At 6 H, a marginal increase in turbidity was observed, particularly at 0.15 M (~19.5 NTU) and 0.5 M (~20 NTU) (Figure 10(e)). By 24 H, turbidity values remained within a narrow range, with ~17.5 NTU recorded at the highest salt concentration (Figure 10(f)), suggesting only minor ionic effects without visible aggregation [37].

The UV–Vis spectra of Bai-CDs (Figures 11(d–f)) showed excellent consistency across all NaCl concentrations. Although a slight spectral shift was observed at 0.5 M NaCl, it did not significantly impact the absorbance profile, indicating minimal nanoparticle clustering. The higher baseline turbidity observed for Bai-CDs compared to CDs is attributed, in part, to baicalein's inherent optical absorbance and light-scattering characteristics. Nonetheless, the absence of significant spectral disruptions confirms that baicalein coating effectively provides steric stabilization, reducing the likelihood of salt-induced aggregation [36].

In summary, both CDs and Bai-CDs maintained strong colloidal and optical stability under increasing ionic strength, making them suitable candidates for physiological applications. The observed differences in turbidity trends between the two formulations reflect their distinct stabilization mechanisms, which is electrostatic for CDs and combined electrostatic steric for Bai-CDs.

3.3.3 Turbidity Analysis

Turbidity measurements served as a key quantitative indicator of colloidal stability, complementing visual and spectroscopic data. For CDs, the highest turbidity values were observed under acidic conditions, particularly at pH 3 and 4, across all time points (Figures 8(a–c)). At 1 H, turbidity peaked sharply at pH 3 (~13 NTU) and remained elevated at 6 H and 24 H (~12 NTU and ~11 NTU, respectively), signifying persistent particle aggregation. These trends correlated well with the visual appearance of precipitation (Figure 7(a)) and the decline in UV–Vis absorbance (Figures 9(a–c)), supporting the conclusion that protonation of surface groups at low pH disrupts electrostatic repulsion and promotes aggregation.

In contrast, CDs demonstrated strong tolerance to ionic strength changes. Across all NaCl concentrations (0–0.5 M), turbidity remained low and stable (Figures 8(d–f)). Slight increases were observed at 0.5 M NaCl, particularly at 6 H (~2.3 NTU) and 24 H (~1.6 NTU), likely due to partial charge screening. However, the lack of visible aggregation or significant changes in UV–Vis spectra (Figures 9(d–f)) confirmed that the colloidal integrity of CDs was well maintained under salt stress.

Bai-CDs exhibited a similar but slightly more complex turbidity pattern. Turbidity was consistently highest at pH 3 across all time intervals, with values reaching ~26 NTU at 1H and remaining elevated through 24 H (Figures 10(a–c)), indicating some degree of acid-induced aggregation. However, from pH 4 to 12, turbidity values progressively decreased over time, suggesting improved dispersion and long-term stability in neutral to basic environments. Interestingly, a secondary turbidity increase was observed at pH 9, possibly linked to subtle interactions between baicalein and surface functional groups at higher pH levels. While this peak did not coincide with visual precipitation or significant absorbance changes, it may reflect conformational or surface rearrangements in the baicalein layer.

Under ionic strength conditions, Bai-CDs displayed moderate but stable turbidity values ranging from ~19 NTU to ~21 NTU across NaCl concentrations and time points (Figures 10(d–f)). Unlike CDs, Bai-CDs maintained relatively higher baseline turbidity throughout the study. This elevation is not necessarily indicative of particle aggregation, but rather an optical artifact attributed to the intrinsic yellow coloration and light-scattering properties of baicalein. UV–Vis spectra across these conditions (Figures 11(d–f)) remained consistent, reinforcing the conclusion that turbidity increases were not solely due to nanoparticle clustering.

Therefore, while turbidity offers useful quantitative insight, its interpretation must consider both compositional and optical properties of the nanoparticles. For Bai-CDs in particular, the higher turbidity values should be cautiously interpreted in the context of baicalein's optical contributions. A holistic assessment combining turbidity, UV–Vis spectral profiles, and visual inspection provides a more accurate evaluation of colloidal stability.

Overall, both CDs and Bai-CDs showed good stability under different pH and salt conditions. CDs were less stable at low pH, while Bai-CDs performed better due to the protective effect of baicalein. Both remained stable in salt solutions, with Bai-CDs showing slightly higher turbidity because of baicalein's color. These findings suggest Bai-CDs are more suitable for drug delivery in physiological environments. A summary of all stability parameters, including comparisons with literature-defined optimal ranges, is presented in Table 1.

This study underscores the importance of understanding environmental factors to optimize the colloidal stability of nanomaterials for practical applications. While CDs alone exhibit broad stability, their vulnerability under acidic conditions can be mitigated through baicalein modification, which enhances stability and makes Bai-CDs more resilient to pH fluctuations [38], [39].

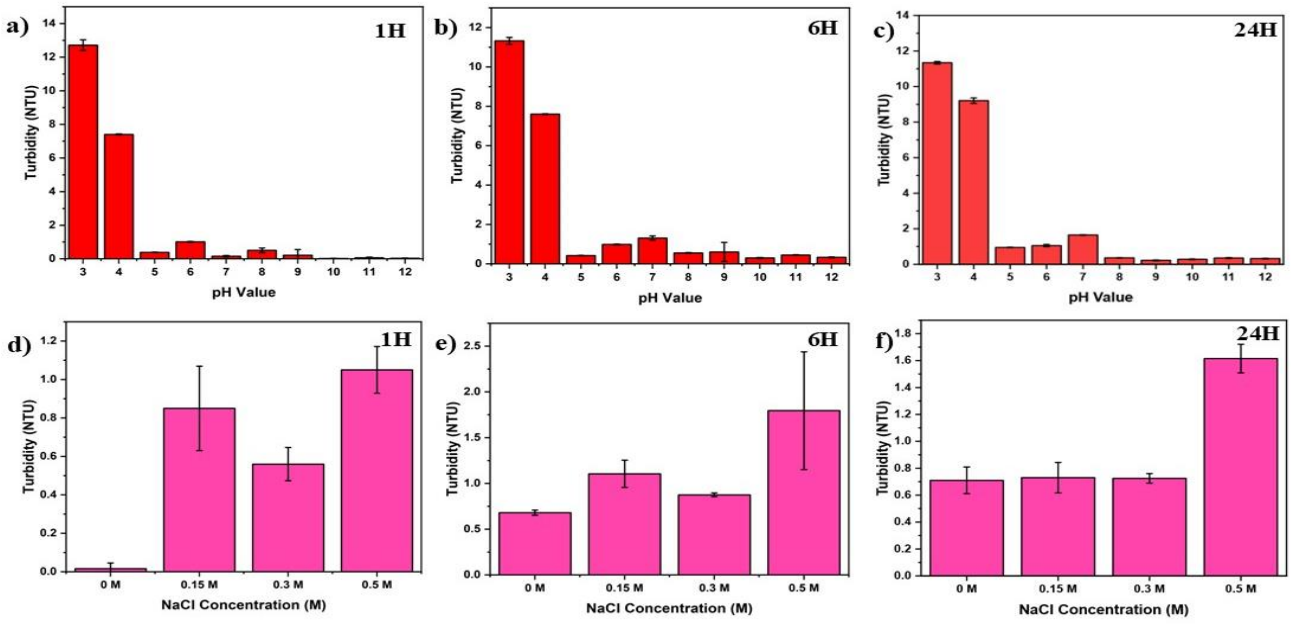

Figure 8 Turbidity measurements of carbon nanodots (CDs) under various pH and ionic strength conditions over time. (a–c) Turbidity (NTU) of CDs dispersed in solutions with different pH values (3–12) after (a) 1 H, (b) 6 H, and (c) 24 H. (d–f) Turbidity of CDs in solutions containing varying NaCl concentrations (0–0.5 M) after (d) 1 H, (e) 6 H, and (f) 24 H

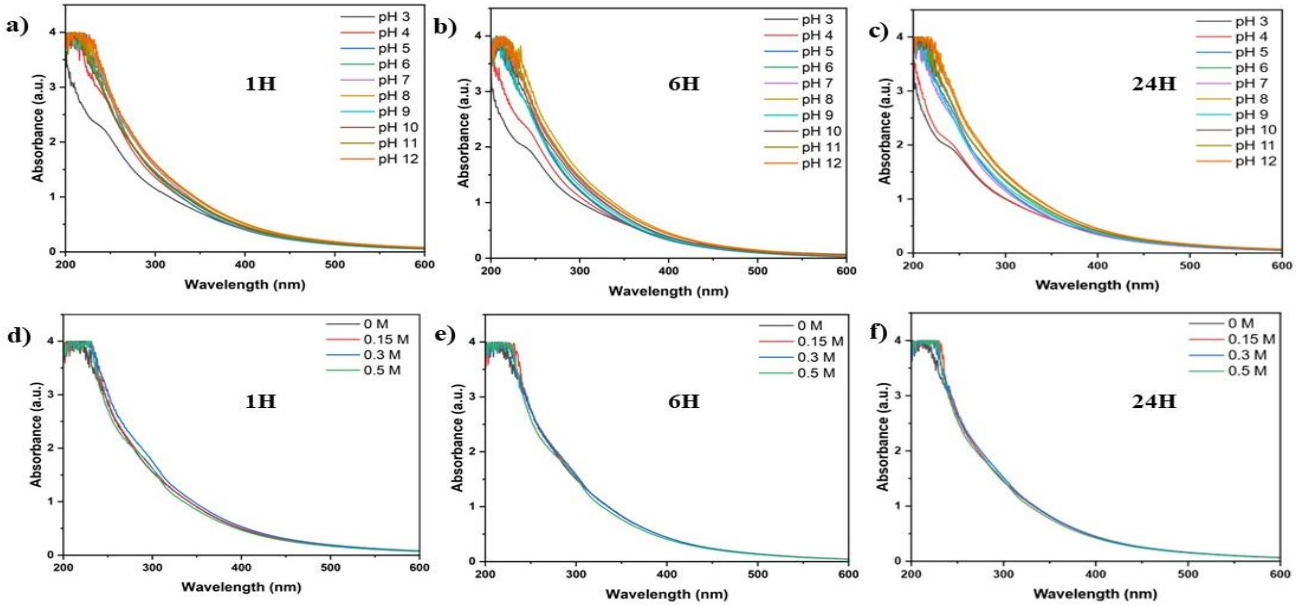

Figure 9 UV-Vis absorption spectra of carbon nanodots (CDs) under varying conditions to assess colloidal stability over time. (a–c) Absorbance profiles of CDs incubated at different pH values (3–12) for (a) 1 H, (b) 6 H, and (c) 24 H. (d–f) Absorbance profiles of CDs at different NaCl concentrations (0 M, 0.15 M, 0.3 M, 0.5 M) for (d) 1 H, (e) 6 H, and (f) 24 H. The spectra reveal the influence of pH and ionic strength on the optical properties and stability of CDs in aqueous media over time

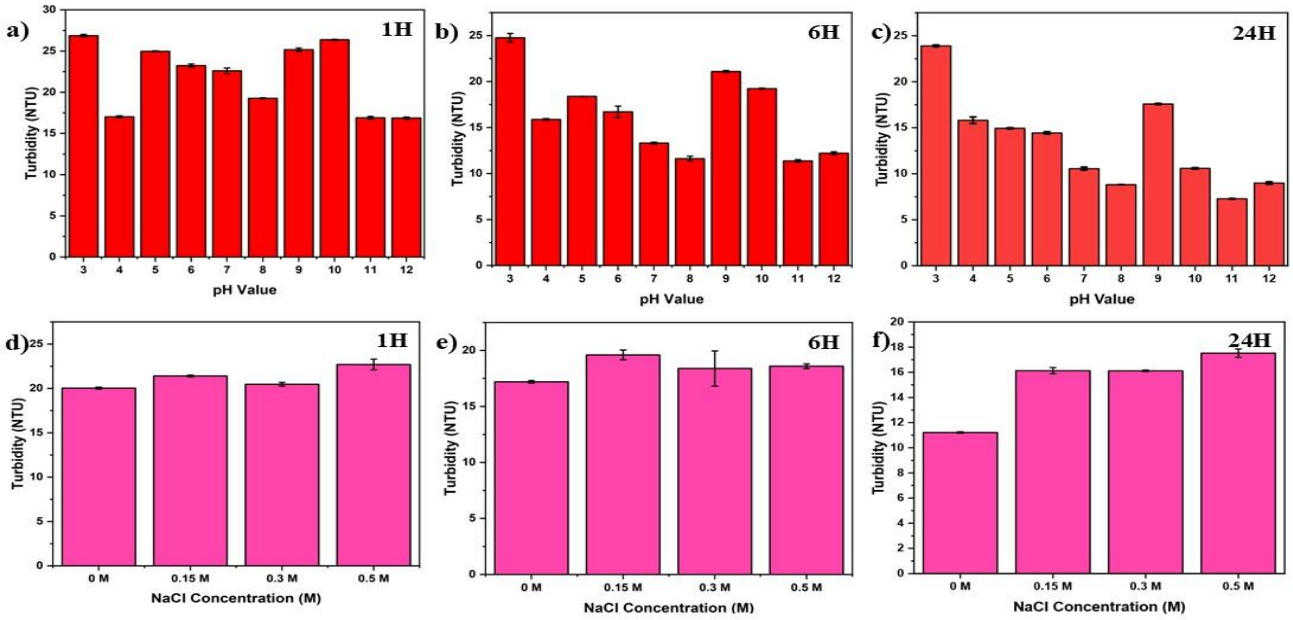

Figure 10 Turbidity measurements of Bai-CDs under various pH and ionic strength conditions over time. (a–c) Turbidity (NTU) of Bai-CDs dispersed in solutions with different pH values (3–12) after (a) 1 H, (b) 6 H, and (c) 24 H. (d–f) Turbidity of Bai-CDs in solutions containing varying NaCl concentrations (0–0.5 M) after (d) 1 H, (e) 6 H, and (f) 24 H

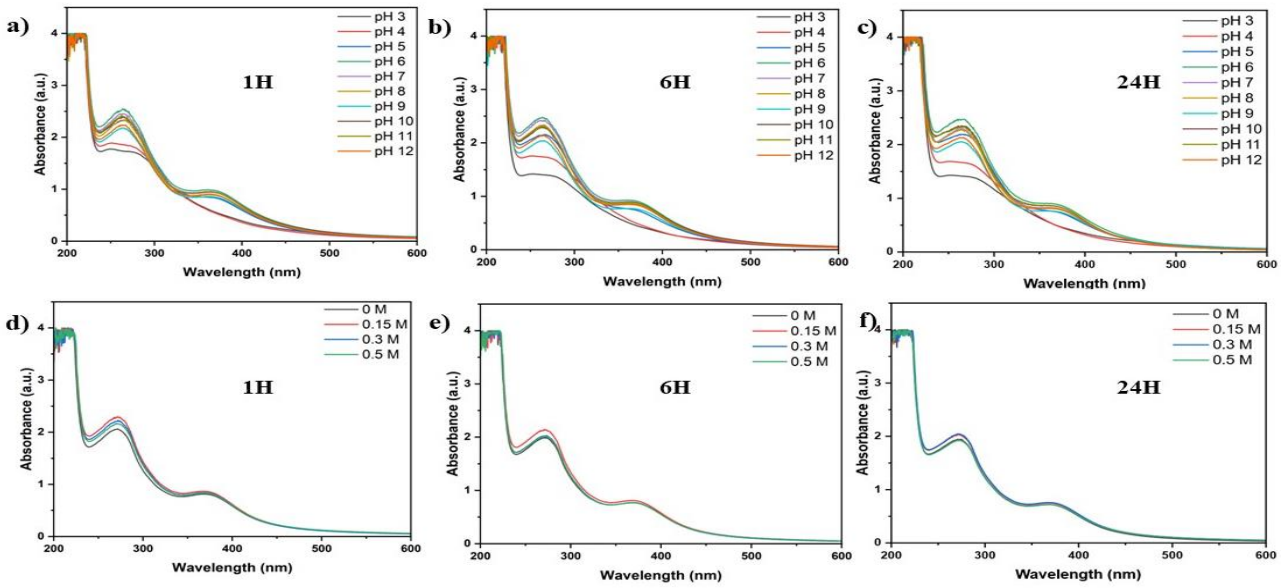

Figure 11 UV-Vis absorption spectra of Bai-CDs under varying conditions to assess colloidal stability over time. (a–c) Absorbance profiles of Bai-CDs incubated at different pH values (3–12) for (a) 1 H, (b) 6 H, and (c) 24 H. (d–f) Absorbance profiles of Bai-CDs at different NaCl concentrations (0 M, 0.15 M, 0.3 M, 0.5 M) for (d) 1 H, (e) 6 H, and (f) 24 H. The spectra reveal the influence of pH and ionic strength on the optical properties and stability of Bai-CDs in aqueous media over time

Table 1 Summary of stability evaluation parameters for CDs and Bai-CDs relevant to drug delivery suitability

Parameter	Optimal range for drug delivery	Observed in CDs	Observed in Bai-CDs
pH stability range	4-9 [33]	5-12 (unstable at pH 3-4)	4-12 (slightly unstable at pH 3)
Salt tolerance (NaCl)	Up to 0.15-0.5M [34]	Stable up to 0.5 M	Stable up to 0.5 M
Aggregation within 24H	Minimal or none [35]	Precipitation at low pH	Delayed aggregation at pH 3
Turbidity	Low to moderate [35]	High at pH 3-4	Elevated due to baicalein color, not aggregation

This improved stability is particularly advantageous for drug delivery systems, where nanoparticles must retain their structural integrity and functionality in diverse biological environments, such as the acidic tumor microenvironment. The incorporation of baicalein onto CDs not only enhances colloidal stability but also provides a synergistic approach to improving drug bioavailability and controlled release. Bai-CDs benefit from a combination of electrostatic and steric stabilization mechanisms. While CDs alone rely on electrostatic repulsion to resist aggregation under varying ionic strength conditions, they are prone instability at low pH due to protonation. In contrast, baicalein modification introduces steric hindrance, reducing sensitivity to both pH and ionic strength variations. These insights highlight the potential of functionalized carbon nanodots in biomedical applications, particularly as effective carriers for targeted cancer therapy.

3.4 Comparative Advantages of Bai-CDs Over Conventional Drug Carriers

Compared to conventional drug delivery systems such as liposomes, Poly (lactic-co-glycolic acid) (PLGA)-based nanoparticles, dendrimers, and other carbon-based nanocarriers like graphene oxide and carbon nanotubes, Bai-CDs offer a suite of unique and superior features that position them as a promising platform for advanced drug delivery applications, particularly in cancer therapy [40].

One of the most compelling advantages of Bai-CDs lies in their exceptional colloidal stability across a wide range of physiological conditions. As demonstrated in Section 3.3, Bai-CDs maintain structural integrity and remain well-dispersed across pH 4 to 12 and up to 0.5 M NaCl, outperforming many polymeric and lipid-based carriers that often undergo aggregation, hydrolysis, or destabilization under acidic or ionic stress conditions commonly found in tumor microenvironments [41]. This robustness ensures reliable delivery and distribution in complex biological systems where conventional carriers frequently underperform.

In addition, Bai-CDs possess intrinsic fluorescence, enabling real-time, label-free bioimaging and tracking of drug distribution and cellular uptake. This feature not only reduces the need for external fluorophores which can complicate synthesis and

raise cytotoxicity risks but also aligns Bai-CDs with the growing field of theranostics, where therapy and diagnostics are integrated into a single nanoplatform. Traditional systems like PLGA or liposomes often require conjugation with external dyes or contrast agents, adding layers of complexity and potential instability [42].

Functionally, the incorporation of baicalein enhances the system beyond passive delivery. Baicalein serves both as the therapeutic payload and as a surface modifier, contributing to steric stabilization while imparting antioxidant, anti-inflammatory, and anticancer properties. This dual-functionality design provides a synergistic therapeutic effect, transforming the carrier itself into a bioactive agent [43].

This is in stark contrast to inert carriers like liposomes or dendrimers, which typically lack inherent biological activity and rely solely on the encapsulated drug for therapeutic action.

Furthermore, Bai-CDs demonstrate favorable biocompatibility and safety profiles, rooted in their carbon-based origin. Unlike metal-based nanoparticles (e.g., gold or silver), which may induce oxidative stress or long-term toxicity, carbon nanodots are well-documented for their low toxicity, high biodegradability, and eco-friendly synthesis particularly when derived from citric acid or plant-based precursors, as in this study [32], [44].

Taken together, the broad environmental stability, inherent fluorescence, bioactive synergy, and excellent biocompatibility of Bai-CDs collectively establish them as a next-generation multifunctional nanocarrier. These characteristics not only overcome the limitations of traditional drug delivery systems but also pave the way for precision medicine approaches in enhancing the bioavailability and therapeutic efficacy of baicalein for targeted cancer treatment.

4.0 CONCLUSION

This study successfully developed baicalein-loaded carbon nanodots (Bai-CDs) as an innovative drug delivery system for cancer therapy. The synthesis and characterization of these nanoparticles demonstrated optimal physicochemical properties, enhancing the solubility and stability of baicalein. Characterization techniques confirmed effective loading and stability under various conditions, indicating their potential for targeted drug delivery.

The findings suggest that Bai-CDs could improve therapeutic outcomes while minimizing toxicity in cancer treatments. This research contributes to the advancement of nanotechnology in drug delivery and paves the way for future studies on their clinical applications.

Acknowledgements

This work was supported by a Universiti Sains Malaysia, Special (Matching) Short-term Grant with Project No: 304/PPSK/6315717.

Conflicts of Interest

The authors declare that there is no conflict of interest regarding the publication of this paper.

References

[1] American Cancer Society. 2019. *Cancer Treatment and Survivorship Facts and Figures 2019–2021*. Atlanta: American Cancer Society. https://www.cancer.org/research/cancer-facts-statistics/survivor-facts-figures.html.

[2] National Cancer Institute. 2018. *Chemotherapy and You*. Bethesda, MD: U.S. Department of Health and Human Services, National Institutes of Health. https://www.cancer.gov/cancertopics/coping/chemotherapy-and-you.

[3] Hoek, J., H. L. van der Weide, T. Dijkema, R. J. H. M. Steenbakkers, L. V. van Dijk, G. H. de Bock, and J. L. N. Roodenburg. 2016. Nephrotoxicity as a Dose-Limiting Factor in a High-Dose Cisplatin-Based Chemoradiotherapy Regimen for Head and Neck Carcinomas. *Cancers.* 8(2): 21. https://doi.org/10.3390/cancers8020021.

[4] Manohar, S., and N. Leung. 2018. Cisplatin Nephrotoxicity: A Review of the Literature. *Journal of Nephrology*. 31(1): 15–25. https://doi.org/10.1007/s40620-017-0392-z.

[5] Zhu, X., H. Zhu, H. Luo, W. Zhang, Z. Shen, and X. Hu. 2016. Molecular Mechanisms of Cisplatin Resistance in Cervical Cancer. *Drug Design, Development and Therapy*. 10: 1885–97. https://doi.org/10.2147/DDDT.S106412.

[6] Iqbal, J., M. Ahmed, Z. Mehmood, M. A. Khan, and W. Qamar. 2017. Plant-Derived Anticancer Agents: A Green Anticancer Approach. *Asian Pacific Journal of Tropical Biomedicine*. 7(12): 1129–50. https://doi.org/10.1016/j.apjtb.2017.10.016.

[7] Liu, H., J. Zhang, F. Wang, L. Li, and Y. Yang. 2016. The Fascinating Effects of Baicalein on Cancer: A Review. *International Journal of Molecular Sciences.* 17(10): 1681. https://doi.org/10.3390/ijms17101681.

[8] Li, K., Y. Wang, J. Zhang, L. Chen, and Y. Liu. 2016. Preparation and Characterization of Baicalein-Loaded Nanoliposomes for Antitumor Therapy. *Journal of Nanomaterials.* 2016: 2861915. https://doi.org/10.1155/2016/2861915.

[9] Qiao, C., R. Wang, X. Yang, Y. Tang, Y. Xia, L. Lin, and J. Zhang. 2016. Oroxylin A Modulates Mitochondrial Function and Apoptosis in Human Colon Cancer Cells by Inducing Mitochondrial Translocation of Wild-Type p53. *Oncotarget* 7(13): 17009–20. https://doi.org/10.18632/oncotarget.7927.

[10] Morshed, A. K. M. H., N. Das, Y. Araf, M. A. Taniya, M. B. Hosen, N. A. Banu, and T. Sultana. 2023. Baicalein as a Promising Anticancer Agent: A Comprehensive Analysis of Molecular Mechanisms and Therapeutic Perspectives. *Cancers.* 15(7): 2128. https://doi.org/10.3390/cancers15072128.

[11] Rahmani, A. H., A. Almatroudi, A. A. Khan, A. Y. Babiker, M. Alanezi, and K. S. Allemailem. 2022. The Multifaceted Role of Baicalein in Cancer Management through Modulation of Cell Signalling Pathways. *Molecules.* 27(22): 8023. https://doi.org/10.3390/molecules27228023.

[12] Mohammed, J., P. K. Desu, J. R. Namratha, and G. K. Rao. 2023. Applications of Carbon Dots (CDs) in Drug Delivery. *Advances in Pharmacology and Pharmacy*. 11(1): 36–45. https://doi.org/10.13189/app.2023.110104.

[13] Parvin, M., M. S. Rahman, M. T. Islam, and M. Hossain. 2022. Oroxylum indicum Stem Bark Extract Reduces Tumor Progression by Inhibiting the EGFR–PI3K–AKT Pathway in an In Vivo 4NQO-Induced Oral Cancer Model. *Journal of the American Nutrition Association*. 1–15. https://doi.org/10.1080/27697061.2022.2107583.

[14] Banger, A., R. Sharma, S. Kumar, and S. Gupta. 2023. Synthetic Methods and Applications of Carbon Nanodots. *Catalysts* 13(5): 858. https://doi.org/10.3390/catal13050858.

[15] Debnath, S. K., and R. Srivastava. 2021. Drug Delivery with Carbon-Based Nanomaterials as Versatile Nanocarriers: Progress and Prospects. *Frontiers in Nanotechnology*. 3(April): 644564. https://doi.org/10.3389/fnano.2021.644564.

[16] Fahmi, M. Z., N. F. Sholihah, A. Wibrianto, S. C. W. Sakti, F. Firdaus, and J. Chang. 2021. Simple and Fast Design of Folic Acid-Based Carbon Dots as a Theranostic Agent and Its Drug Release Aspect. *Materials Chemistry and Physics*. 267: 124596. https://doi.org/10.1016/j.matchemphys.2021.124596.

[17] Romero, M. P., D. González, E. Pérez, and M. Díaz. 2021. One-Pot Microwave-Assisted Synthesis of Carbon Dots and In Vivo and In Vitro Antimicrobial Photodynamic Applications. *Frontiers in Microbiology*. 12(June): 662149. https://doi.org/10.3389/fmicb.2021.662149.

[18] Bhaisare, M. L., A. Talib, M. S. Khan, S. Pandey, and H.-F. Wu. 2015. Synthesis of Fluorescent Carbon Dots via Microwave Carbonization of Citric Acid in the Presence of Tetraoctylammonium Ion and Their Application to Cellular Bioimaging. *Microchimica Acta*. 182(13–14): 2173–81. https://doi.org/10.1007/s00604-015-1541-5.

[19] Kong, D., F. Yan, Z. Han, J. Xu, X. Guo, and L. Chen. 2016. Cobalt(II) Ions Detection Using Carbon Dots as a Sensitive and Selective Fluorescent Probe. *RSC Advances*. 6(72): 67481–87. https://doi.org/10.1039/C6RA12986B.

[20] Dong, G., X. Zhang, Y. Liu, J. Wu, and Y. Yang. 2020. Facile Synthesis of N,P-Doped Carbon Dots from Maize Starch via a Solvothermal Approach for Highly Sensitive Detection of Fe^{3+}. *RSC Advances*. 10(55): 33483–89. https://doi.org/10.1039/D0RA06209J.

[21] Feiner, I. V. J., J. Rojas, H. Yang, J. Lee, and S. Park. 2021. Pre-Targeting with Ultra-Small Nanoparticles: Boron Carbon Dots as Drug Candidates for Boron Neutron Capture Therapy. *Journal of Materials Chemistry B*. 9(2): 410–20. https://doi.org/10.1039/D0TB01880E.

[22] Arvapalli, D. M., A. T. Sheardy, K. Allado, H. Chevva, Z. Yin, and J. Wei. 2020. Design of Curcumin-Loaded Carbon Nanodots Delivery System: Enhanced Bioavailability, Release Kinetics, and Anticancer Activity. *ACS Applied Bio Materials*. 3(12): 8776–85. https://doi.org/10.1021/acsabm.0c01144.

[23] Zuo, D., N. Liang, J. Xu, D. Chen, and H. Zhang. 2019. UV Protection from Cotton Fabrics Finished with Boron- and Nitrogen-Co-Doped Carbon Dots. *Cellulose*. 26(6): 4205–12. https://doi.org/10.1007/s10570-019-02365-5.

[24] Wibrianto, A., S. Q. Khairunisa, S. C. W. Sakti, Y. L. Ni'mah, B. Purwanto, and M. Z. Fahmi. 2021. Comparison of the Effects of Synthesis Methods of B-, N-, S-, and P-Doped Carbon Dots with High Photoluminescence Properties on HeLa Tumor Cells. *RSC Advances*. 11(2): 1098–1108. https://doi.org/10.1039/D0RA09403J.

[25] Sun, Y., S. Bi, D. Song, C. Qiao, D. Mu, and H. Zhang. 2008. Study on the Interaction Mechanism between DNA and the Main Active Components in *Scutellaria baicalensis* Georgi. *Sensors and Actuators B: Chemical*. 129(2): 799–810. https://doi.org/10.1016/j.snb.2007.09.082.

[26] Roy, A. S., A. K. Dinda, N. K. Pandey, and S. Dasgupta. 2016. Effects of Urea, Metal Ions, and Surfactants on the Binding of Baicalein with Bovine Serum Albumin. *Journal of Pharmaceutical Analysis* 6(4): 256–67. https://doi.org/10.1016/j.jpha.2016.04.001.

[27] Das, R., G. Rajender, and P. K. Giri. 2018. Anomalous Fluorescence Enhancement and Fluorescence Quenching of Graphene Quantum Dots by Single-Walled Carbon Nanotubes. *Physical Chemistry Chemical Physics*. 20(6): 4527–37. https://doi.org/10.1039/C7CP06994D.

[28] Pahang, F., P. Parvin, and A. Bavali. 2020. Fluorescence Quenching Effects of Carbon Nanostructures (Graphene Oxide and Nanodiamond) Coupled with Methylene Blue. *Spectrochimica Acta Part A: Molecular and Biomolecular Spectroscopy*. 229: 117888. https://doi.org/10.1016/j.saa.2019.117888.

[29] Xu, J., *et al.* 2012. Efficient Fluorescence Quenching in Carbon Dots by Surface-Doped Metals—Disruption of Excited State Redox Processes and Mechanistic Implications. *Langmuir*. 28(46): 16141–47. https://doi.org/10.1021/la302506e.

[30] Serag, E., M. Helal, and A. El Nemr. 2024. Curcumin Loaded onto Folic Acid Carbon Dots as a Potent Drug Delivery System for Antibacterial and Anticancer Applications. *Journal of Cluster Science*. 35(2): 519–32. https://doi.org/10.1007/s10876-023-02491-y.

[31] Zhou, Y., *et al.* 2017. A Novel Matrix Dispersion Based on Phospholipid Complex for Improving Oral Bioavailability of Baicalein: Preparation, In Vitro and In Vivo Evaluations." *Drug Delivery*. 24(1): 720–28. https://doi.org/10.1080/10717544.2017.1311968.

[32] Lin, Z., *et al.* 2022. Citric Acid-Derived Carbon Dots as Excellent Cysteine Oxidase Mimics for Cysteine Sensing. *Sensors and Actuators B: Chemical*. 359: 131563. https://doi.org/10.1016/j.snb.2022.131563.

[33] Abdella, S., *et al*. 2023. pH and Its Applications in Targeted Drug Delivery. *Drug Discovery Today*. 28(1): 103414. https://doi.org/10.1016/j.drudis.2022.103414.

[34] Baral, K. C., *et al.* 2021. Enhanced Bioavailability of AC1497, a Novel Anticancer Drug Candidate, via a Self-Nanoemulsifying Drug Delivery System. *Pharmaceutics*. 13(8): 1142. https://doi.org/10.3390/pharmaceutics13081142.

[35] Kwee, Y., A. N. Kristanti, N. S. Aminah, and M. Z. Fahmi. 2020. Design of Catechin-Based Carbon Nanodots as Facile Staining Agents of Tumor Cells. *Indonesian Journal of Chemistry*. 20(6): 1332. https://doi.org/10.22146/ijc.50327.

[36] Qin, J., *et al.* 2021. pH Sensing and Bioimaging Using Green Synthesized Carbon Dots from Black Fungus. *RSC Advances*. 11(50): 31791–94. https://doi.org/10.1039/D1RA05199G.

[37] Song, J., A. S. Vikulina, B. V. Parakhonskiy, and A. G. Skirtach. 2023. Hierarchy of Hybrid Materials. Part II: The Place of Organics-on-Inorganics in It, Their Composition and Applications. *Frontiers in Chemistry*. 11: 1078840. https://doi.org/10.3389/fchem.2023.1078840.

[38] Dua, S., P. Kumar, B. Pani, M. Khanna, and G. Bhatt. 2023. Stability of Carbon Quantum Dots: A Critical Review. *RSC Advances*. 13(23): 13845–61. https://doi.org/10.1039/D2RA07180K.

[39] Kong, J., *et al.* 2024. Carbon Quantum Dots: Properties, Preparation, and Applications. *Molecules*. 29(9): 2002. https://doi.org/10.3390/molecules29092002.

[40] Tabatabaei Mirakabad, F. S., *et al.* 2014. PLGA-Based Nanoparticles as Cancer Drug Delivery Systems. *Asian Pacific Journal of Cancer Prevention*. 15(2): 517–35. https://doi.org/10.7314/APJCP.2014.15.2.517.

[41] Mehta, M., T. A. Bui, X. Yang, Y. Aksoy, E. M. Goldys, and W. Deng. 2023. Lipid-Based Nanoparticles for Drug/Gene Delivery: An Overview of the Production Techniques and Difficulties Encountered in Their Industrial Development. *ACS Materials Au*. 3(6): 600–19. https://doi.org/10.1021/acsmaterialsau.3c00032.

[42] Cohen, E. N., P. P. D. Kondiah, Y. E. Choonara, L. C. du Toit, and V. Pillay. 2020. Carbon Dots as Nanotherapeutics for Biomedical Application. *Current Pharmaceutical Design* 26 (19): 2207–21. https://doi.org/10.2174/1381612826666200402102308.

[43] Zhou, Y., *et al.* 2017. A Novel Matrix Dispersion Based on Phospholipid Complex for Improving Oral Bioavailability of Baicalein: Preparation, In Vitro and In Vivo Evaluations. *Drug Delivery* 24 (1): 720–28. https://doi.org/10.1080/10717544.2017.1311968.

[44] Luo, D., X. Wang, C. Burda, and J. P. Basilion. 2021. Recent Development of Gold Nanoparticles as Contrast Agents for Cancer Diagnosis. *Cancers*. 13(8): 1825. https://doi.org/10.3390/cancers13081825.